J. Inst. Eng. India Ser. C (February 2023) 104(1):219–230
https://doi.org/10.1007/s40032-022-00893-x

REVIEW PAPER

# Tool Edge Preparation Based on Gas–Solid Two-Phase Abrasive Flow

**Yin Yuan[1] · Xuefeng Zhao[1] · Ke You[1]**

Received: 10 May 2022 / Accepted: 4 October 2022 / Published online: 1 November 2022


**Abstract** Edge preparation can prolong the tool life by enhancing cutting process stability and machining quality. In this work, a gas–solid two-phase abrasive flow method for edge preparation was proposed. First, relying on the particle dynamics theory and discrete element theory of gas–solid two-phase flow, a simulation model is developed to study the preparation process via CFD and EDEM coupling method. Likewise, the influences of inlet velocity, the ratio of tool positive and negative rotation time, and the ratio of the tool rotation radius to the revolution radius, the ratio of tool positive and negative rotation speed on the corresponding abrasive speed, force and wear quantity are studied. Additionally, an experimental platform for tool edge preparation based on gas–solid two-phase abrasive flow was established. Moreover, the orthogonal experiments are designed for the shape factor values of $K<1$ and $K>1$, before preparation. Correspondingly, the effects of intake velocity, time ratio, radius ratio and speed ratio, intake pressure on the relevant asymmetric edge form factor are also studied. The experimental results reveal the removal of microscopic defects on the edge surface after preparation, hence validating the feasibility of gas–solid two-phase abrasive flow for edge preparation and demonstrating the formation mechanism of asymmetric cutting.

**Keywords** Gas–solid two-phase abrasive flow · Edge preparation · Form factor · EDEM–Fluent coupling

✉ Xuefeng Zhao
zxf801112@163.com

[1] Mechanical Engineering College, Guizhou University, Guiyang 550025, China

## Introduction

With the ever-increasing requirements for surface quality and accuracy, a more extensive approach is required to investigate the tool edge preparation methods involved in a machining process. Edge preparation can elevate the tool life, realize stable cutting process and high machining quality and thus help to fulfill the requirements of high-speed, high-precision and ultra-precision metal cutting process.

The current research on edge preparation primarily focuses on the influence of edge preparation on corresponding cutting performance, while the development of novel/innovative methods for edge preparation mechanism is generally overlooked. Common methods for edge preparation mainly include nylon brush abrasive preparation of Geber, dry sand blasting preparation of SGT, wet sand blasting preparation of Graf, drag finishing of OTEC and magnetic powder preparation of Magnet Finish [1]. Edge preparation methods are different, and the corresponding mechanisms are also different. In one work, Wang [2] used wet abrasive jet processing, grinding and finishing to prepare the tools and conducted cutting experiments, which demonstrated a good surface and long tool life achieved from wet abrasive jet processing. Similarly, Uhlmann [3] studied the relationship between preparation time and circle radius. Moreover, the drag finishing was utilized to prepare the edge of milling tool, where the results indicated an improvement in tool life and slowing down of tool wear with edge radius through experiments.

The cutting edges are mainly categorized into two subcategories, i.e., symmetric edges or asymmetric edges. The asymmetric edge cannot be reduced to a circle, and it is not precise to describe the edge profiles using only a circle radius. Likewise, the asymmetric edges are usually characterized by a form factor $K$ [4]. Denkena [5] used abrasive nylon brush method to prepare the edge of Physical Vapor Deposition-coated carbide tool. And the shape factor was proposed to characterize the complex asymmetrical edges, as shown in Fig. 1. The symmetrical ($K=1$) and asymmetrical ($K=2$) cutting edges were studied by changing the contact conditions of abrasive brush and work piece. Consequently, the results displayed that asymmetrical cutting edge ($K=2$) suffers least wear, while the symmetrical cutting edge ($K=1$) corresponds to higher cutting force and hence more wear.

This work proposes a gas–solid two-phase abrasive flow machining method for edge preparation. The proposed method is based on drag finishing which is a widely used process for edge preparation and work piece polishing. In drag finishing process, the groups of tools perform planetary motion in grinding abrasives to realize edge preparation. Additionally, the drag finishing method usually adopts stationary dispersed solid abrasives [3]. However, in gas–solid two-phase abrasive flow preparation method, the abrasive is in a state of flow and tools perform two-stage planetary motion in the flow abrasive. Such mechanism reduces the friction between tool and abrasive particles and thus reduces the driving device which inserts into abrasives and moves the tool in stationary grinding particles for a better application prospect. Nevertheless, the current literature lacks in providing experimental studies on edge preparation mechanism with drag finishing method. Therefore, to overcome these gaps, the authors have studied the mechanism of gas–solid two-phase abrasive flow edge preparation.

Current research on gas–solid two-phase flow machining method is limited to only numerical simulations, where Lagrangian particle orbit model is the most widely used model for particle phase simulations. Likewise, gas phase flow field solution models predominantly consist of direct numerical simulation, large vortex simulation, two-equation model, vortex method model and Lattice Boltzmann (LB) method simulation [6]. Similarly, Walther [7] considered vortex stretching effect, turbulent viscosity and turbulence

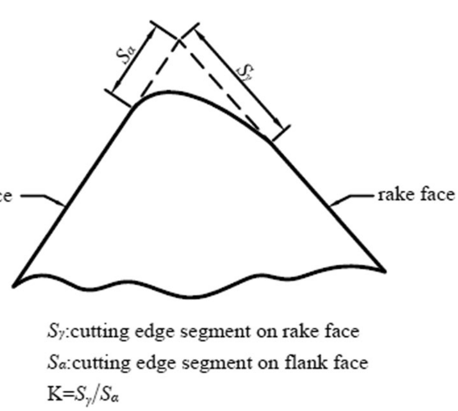


**Fig. 1** Tool edge shape factor *K* characterization method

on the wake of solid phase particles. A three-dimensional viscosity turbulence method was studied, and particle viscosity of turbulence in suspended objects was simulated. The obtained experimental results were consistent with other standard turbulence methods. In another work, Filippova [8] utilized LB method to conduct a three-dimensional gas–solid two-phase flow simulation, analyze the object flow field information and solve object particles equations motion, which revealed the dynamic characteristics of object particles. Furthermore, Ladd [9] proposed a mathematical model using Boltzmann equation to analyze the simulated discrete suspension objects of Brownian particles in uniform airflows. Mass distribution changes of Brownian particles and the particle sediment mass distribution changes of non-discrete spherical Brownian particles in a uniform airflow were investigated. Recently, Junye [10] combined the CFD and EDEM to compare fluid and particle distribution states under different inlet speeds. The results revealed an intense friction, collision effect of the particles and part surface, with an increase in inlet speed. Moreover, the particle kinetic energy was transformed into cutting energy, which in turn improved the material removal rate.

In one work, Miko [11] conducted finishing experiments on twist drills to study the relevant parameters affecting the blunt circle radius in the preparation process of twist drills' cutting edge and established a mathematical model for the blunt circle radius. In another work, Biermann [12] proposed a robot-guided water-jet abrasive machining method for tool passivation and verified the feasibility of the method based on experiments. Recently, Bergs [13] used the preparation method of diamond-coated brush to carry out the preparation test of cemented carbide tools. Similarly, Ventura [14] passivated the PCBN tool through grinding and conducted cutting experiments, and the results showed that the asymmetric edge morphology could improve the tool life. At the same time, Asad [1] obtained tools with different edge profiles by honing and chamfering passivation and used finite element simulation method to simulate various combinations of the feed rate and cutting speed of the edge profile, which laid a foundation for optimizing the tool edge profile and selecting the best cutting parameters. However, Wang [15] adopted Fluent–EDEM coupling simulation to simulate the position information and motion of solid particles in the tank based on the Lagrange particle orbit model and obtained the motion trajectory of a single particle. At the same time, in the simulation setting, the description of fluid motion generally includes three modes: $K-\omega$ two-equation mode, achievable $K-\omega$ two-equation mode and standard $K-\omega$ two-equation mode. The third mode is used as the flow field motion turbulence model of gas–solid two-phase abrasive flow passivation tool [16].

However, gas–solid two-phase abrasive flow for edge preparation is yet to be reported in the literature. The applications of gas–solid two-phase particle flow are merely concentrated in finishing process and single shape of air–solid grinding particle flow on material removal by numerical simulation on particle impact angle.

Therefore, gas–solid two-phase abrasive flow method for edge preparation is proposed in this work. Based on the gas–solid two-phase flow abrasive dynamics theory and discrete element theory, the simulation model of edge preparation process was established by using the software framework (CFD and EDM coupling). The influence of intake velocity, time ratio, radius ratio on abrasive flow state, edge action forces and wear amount is studied. Moreover, an experimental platform for edge preparation based on gas–solid two-phase abrasive flow is established. Through the orthogonal experiments, the influence of preparation time, time ratio, radius ratio, intake pressure and speed ratio on the corresponding form factor is studied for form factor values of $K > 1$ and $K < 1$, before edge preparation. The obtained results from this work highlight an innovative method for edge preparation and lay foundations for high-speed and high-efficient cutting machining.

## Simulation Model Establishment

### Edge Preparation Equipment

Figure 2 illustrates the gas–solid two-phase abrasive flow preparation equipment used in this work for experiments. The equipment is mainly composed of a control part, the abrasive barrel and an air compressor. The tool is installed on a fixture of control part, where it performs a two-stage planetary movement. The abrasive barrel is filled with silicon carbide and brown corundum abrasive. The barrel bottom has a certain number of uniform small holes where each hole is connected with an air compressor via air pipe. The air compressor continuously inputs air into abrasive grain barrel to fluidize the abrasive in a barrel. Every single abrasive exhibits periodic reciprocating motion in the abrasive barrel. However, all abrasives in the barrel stay in a relatively stable state. Moreover, the airflow is continuously blown into barrel from the bottom mesh screen. Hence, during preparation process, the abrasives accumulated on the bottom of a barrel are subjected to airflow lift force, gravity and an interaction force between the abrasive particles. During the two-stage planetary motion, tool continuously collides with abrasive particles to complete the edge preparation.

**Fig. 2** Gas–solid two-phase abrasive flow preparation equipment

### Simulation Model Establishment

The coupled CFD and EDEM simulation model is viewed in Fig. 3, whereas the tool trajectory equation is mathematically expressed by Eq. (1). During the overall process, a single tool can realize both rotational and revolution movements. Accordingly, a group of tools can also realize both rotational and revolution movements. $R_1$, $R_2$, $R_3$ are the revolution radius of the group abrasive, revolution radius of a single abrasive and rotation radius of a single abrasive, respectively. Lastly, the parameters $\omega_1$, $\omega_2$, $\omega_3$ indicate the corresponding angular velocities. The abrasive barrel is a cylindrical container with a mesh screen at the bottom, and the air flow is constantly blown into the mesh screen at the bottom. In the edge preparation process, the abrasive particles accumulated at the bottom of the barrel are subjected to the lift force of the air flow, their own gravity and the interaction between the abrasive particles and the abrasive particles. The single abrasive particles will show periodic reciprocating motion in the barrel, and all the abrasive particles in the barrel are in a relatively stable state. In the process of two-stage planetary motion, the tool will constantly collide with the abrasive particles to achieve the purpose of edge preparation.

$$\begin{cases} x = R_1 \sin(\omega_1 t) + R_2 \sin(\omega_2 t) + R_3 \sin(\omega_3 t) \\ y = R_1 \cos(\omega_1 t) + R_2 \cos(\omega_2 t) + R_3 \cos(\omega_3 t) \end{cases} \tag{1}$$

In the simulation process, the following components are defined:

(1) The cutting tool is cemented carbide end milling tool.

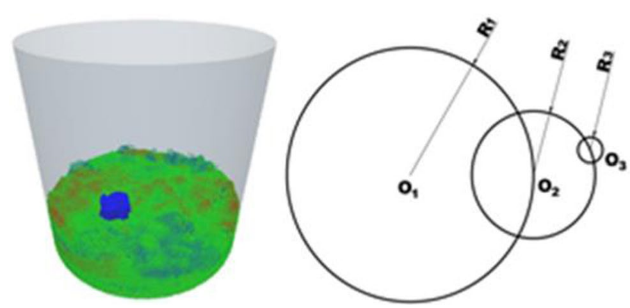


**Fig. 3** Fluent and EDEM simulation model

(2) The diameter and height of abrasive barrel are both 60 mm each, while the diameter of uniform holes at bottom is 0.3 mm with the spacing of 0.5 mm in between them.
(3) The key physical parameters can be directly queried through the database [17]. Parameters for discrete element simulation are tabulated in Table 1.
(4) The Hertz–Mindin with Archard wear model is selected as an interaction model between the particles and solid walls. In this model, both normal and tangential force have damping components where corresponding damping number is related to the coefficient of restitution [18].
(5) The inlet and outlet boundaries are defined as velocity inlet and pressure outlet, respectively. According to calculation of fluid mechanics theory, the turbulence intensity is set to 5%.
(6) The standard $K - \omega$ two-equation model is used as a turbulence model for flow field motion [16].

### EDEM–Fluent Coupling Solution Process Based on DDPM Model

In this paper, EDEM and Fluent are used for coupling. Dense discrete phase model (DDPM) is used in Fluent. The EDEM–Fluent coupling process is a bidirectional data transient transmission process. First of all, the pre-EDEM setting and the pre-Fluent setting are, respectively, carried out. Then, Fluent reads the compiled coupling file and conducts the coupling link through the coupling interface of EDEM. When solving the Fluent software to calculate the flow field of a time step, after EDEM calculating step automatically start the same time, through the interaction of particles and fluid coupling interface, the flow field information, fluid effect of particles and particle information (position, movement, etc.) loop iteration step by step and realize the whole process of the transient simulation.

**Table 1** Main parameters for simulation

| Parameter | Tools | Abrasive |
|---|---|---|
| Static friction coefficient | 0.5 | 0.25 |
| Rolling friction coefficient | 0.01 | 0.01 |
| Restitution Coefficient | 0.5 | 0.75 |
| Density (kg/m$^3$) | 1456 | 3200 |
| Poisson's ratio | 0.3 | 0.14 |
| Shear modulus (Pa) | $2.346 \times 10^{11}$ | $1.796 \times 10^{11}$ |
| Wear constant | $2 \times 10^{-13}$ | – |

## Simulation Results and Analysis

During an edge preparation process, intake velocity, radius ratio (R1:R2) and time ratio (tool forward and reverse motion time) affect the relevant abrasive state, action force and the wear amount.

### Influence of Intake Velocity on Abrasive Motion

The abrasives movement state for the intake velocity of 1 m/s and preparation time 0–0.7 s is shown in Fig. 4. During the initial 0.2 s, abrasives rise sharply and then settle to a certain height where they move in a relatively stable manner.

Likewise, the effect of intake velocity on corresponding abrasive speed is viewed in Fig. 5. The velocity of abrasives increases abruptly in first 0.2 s, while later on, the abrasive fluctuates within a certain speed range. The initial abrasive grains are accumulated at barrel bottom and the gap between the abrasives is small. However, as airflow drives the abrasives to move in an instant state, the gap between the abrasives increases and relevant wind resistance decreases. Correspondingly, the abrasives reach a relatively stable state under continuous airflow action.

### Influence of Preparation Parameters on the Edge Action Force

(1) Influence law of intake velocity on the edge action force

The effects of the intake velocity on edge force are demonstrated in Figs. 6 and 7. Under different values of intake velocity, normal action force fluctuates within a certain range, whereas, with an increase in intake velocity, the fluctuation range becomes larger. Similarly, the tangential force also fluctuates within a certain range, but fluctuation interval shows no obvious correlation with intake velocity. A comparison between the normal and tangential force reveals that normal action force is greater than the tangential force. Hence, the material removal primarily takes place in normal force action.

(2) Influence law of radius ratio on the edge action force

Figures 8 and 9 illustrate the influence of radius ratio on corresponding action force. Under different radius ratio conditions, the normal and tangential forces both oscillate within a certain range where the normal action force is greater than tangential force. Thus, effects of radius ratio change in a process are insignificant because the material removal is substantially stemming from normal force work.

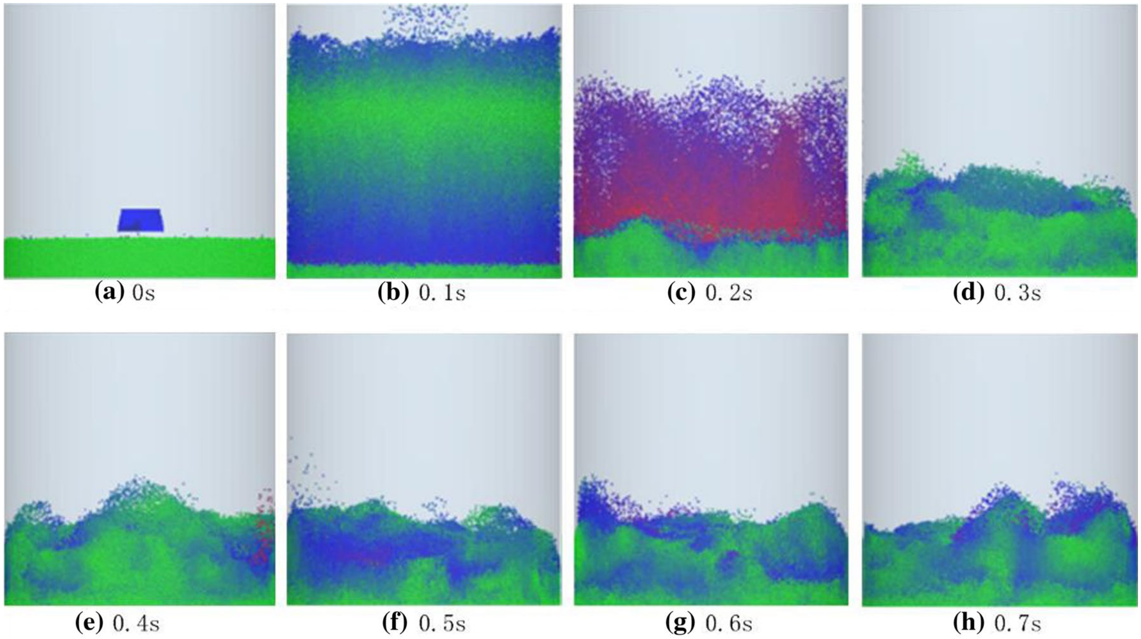


**Fig. 4** Abrasive movement state

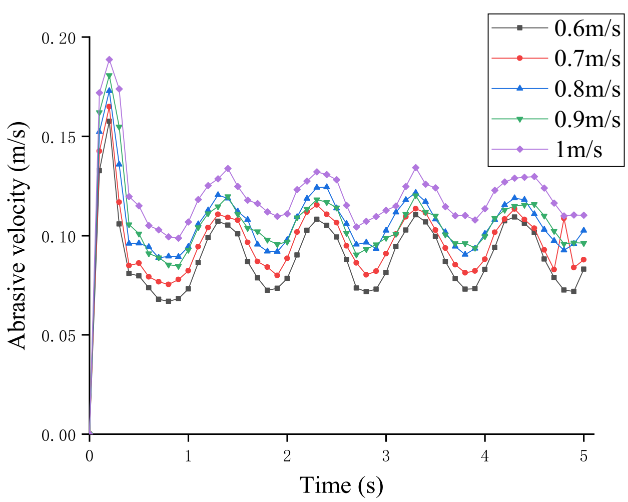


**Fig. 5** Influence of intake velocity on the abrasive velocity

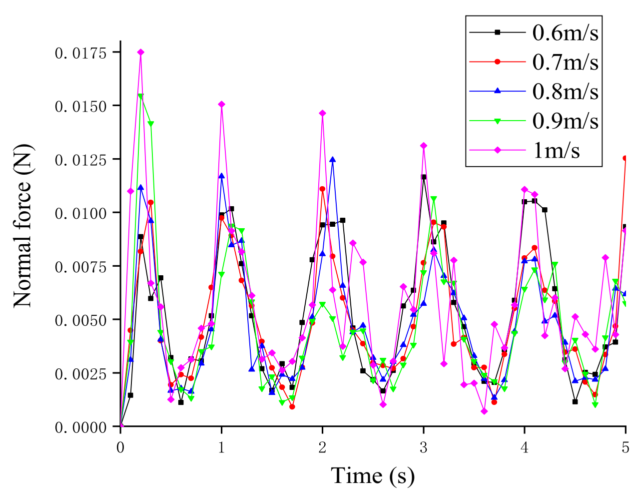


**Fig. 6** Influence law of intake velocity on the normal force

(3) Influence law of time ratio on the edge action force

The influence of time ratio on the action force is plotted in Figs. 10 and 11. As the tool reversal time decreases and tool rotation time increases, the normal force fluctuation range gets smaller. However, the normal force in this case still dominates over tangential force.

## Influence of Preparation Parameters on the Wear Amount

(1) Influence law of intake velocity on the wear amount

Influence law of intake velocity on the wear amount of cutting edge is presented in Fig. 12. It can be seen that wear amount increases with increasing intake velocity, since the large intake velocity results in higher abrasive velocity. Likewise, high abrasive velocity corresponds to larger

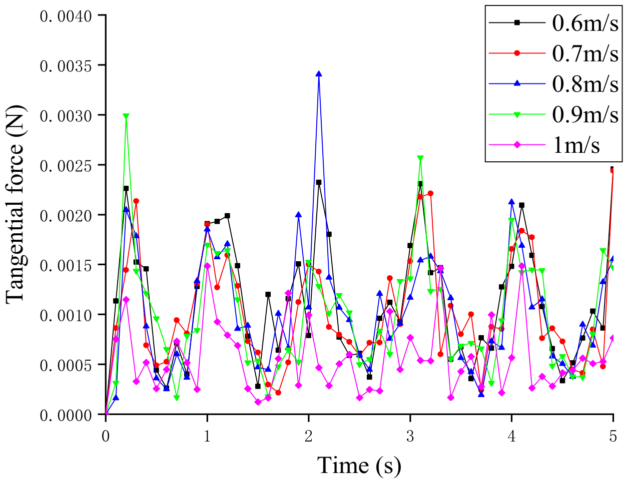


**Fig. 7** Influence law of intake velocity on the tangential force

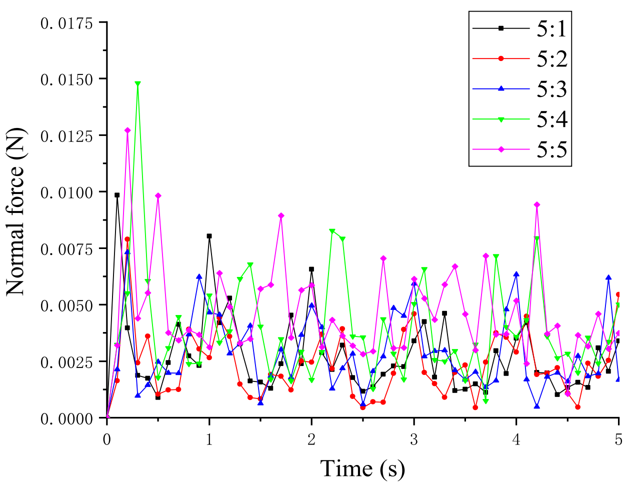


**Fig. 8** Influence law of radius ratio on the normal force

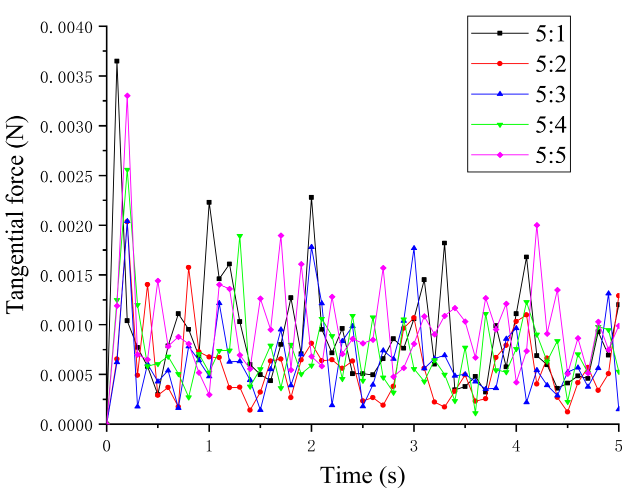


**Fig. 9** Influence law of radius ratio on the tangential force

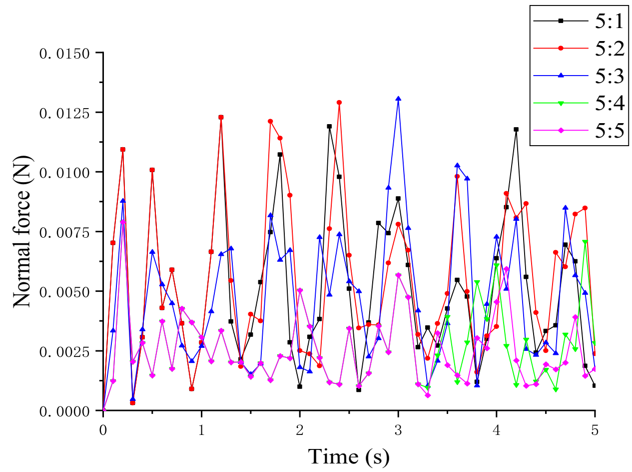


**Fig. 10** Influence law of time ratio on the normal force

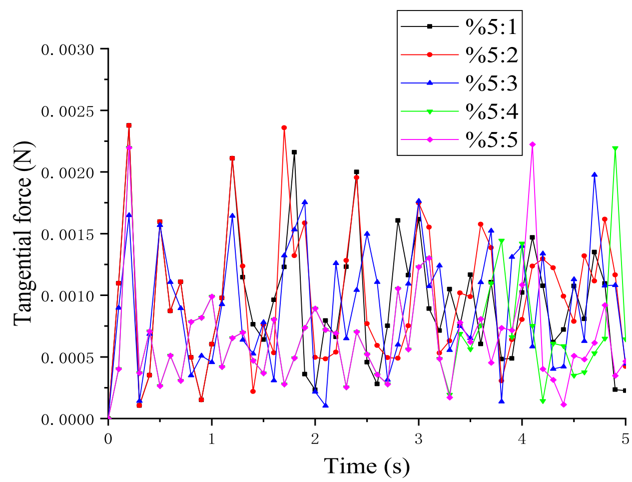


**Fig. 11** Influence law of time ratio on the tangential force

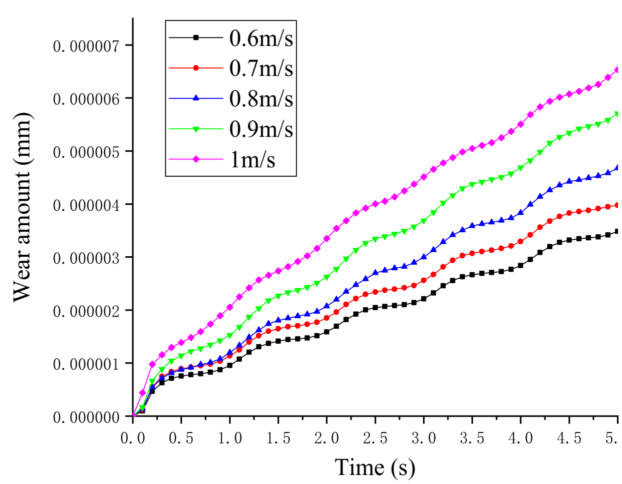


**Fig. 12** Influence of intake velocity on the wear amount

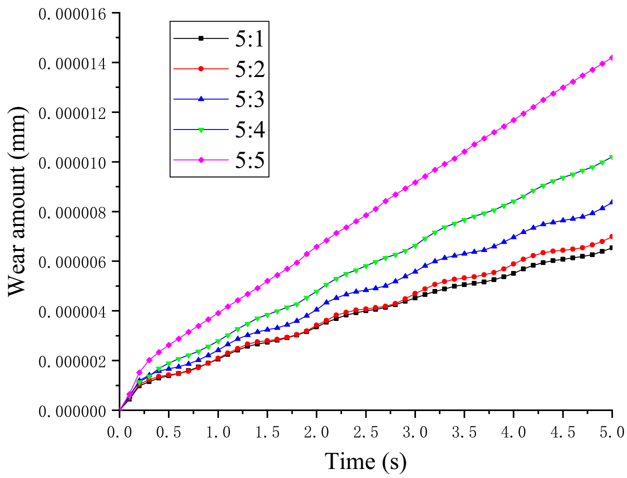


**Fig. 13** Influence of radius ratio on the wear amount

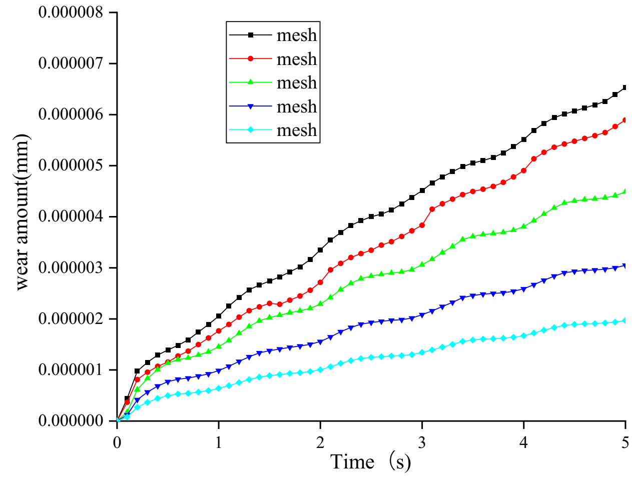


**Fig. 15** Influence of abrasive mesh on the wear amount

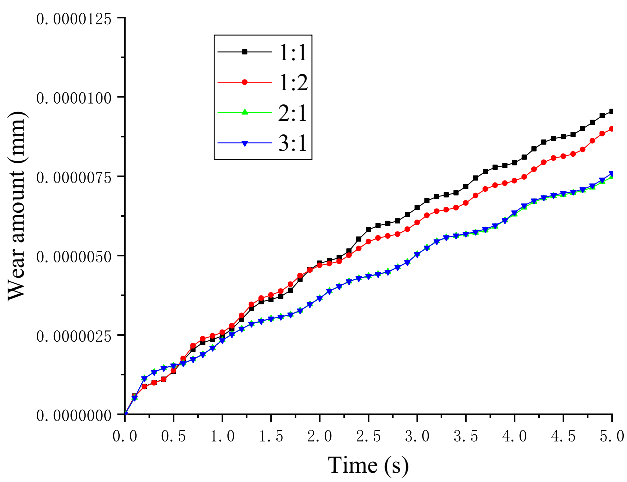


**Fig. 14** Influence of time ratio on the wear amount

**Fig. 16** Milling tool

abrasive impact on the cutting edge and hence the greater wear amount.

(2) Influence law of radius ratio on the wear amount

The influence law of radius ratio on cutting edge wear amount is shown in Fig. 13. An increase in rotation radius R2 expands the volume swept by cutting edge and simultaneously increases the impact number. At radius ratio of 5:5, impact on the edge is highly uniform, and the relevant obtained wear amount is maximum. Thus, an increase in rotation radius R2 directly increases the corresponding wear amount.

(3) Influence law of time ratio on the wear amount

Progressively, influence of time ratio on the respective wear amount is observed in Fig. 14. While the forward rotation time is less than or equal to reverse rotation time, wear amount decreases with the increase in reverse rotation time. On the contrary, for values of forward rotation time greater than reverse rotation time, the wear amount increases marginally with increasing forward rotation time.

(4) Influence law of abrasive mesh on the wear amount

Finally, the influence of abrasive mesh on the corresponding wear amount is displayed in Fig. 15. It can be observed that wear amount increases with the increasing mesh. Since mesh increases under the condition of constant total mass, volume of a single abrasive is reduced and the total number of abrasives increase. Consequently, the impact times increase, hence increasing the wear amount.

## Experimental Results

### Orthogonal Experiment Scheme

For experiments, the used cutting tool possesses a cemented carbide end mill (Fig. 16). The cutting edges can be either symmetric or asymmetric edges; however, the preparation

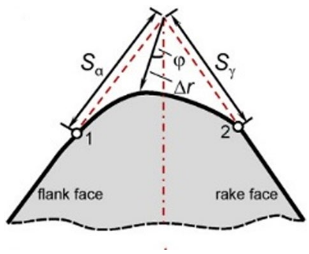


**Fig. 17** Asymmetric edges characterization

**Fig. 18** Edge morphology before edge preparation

**Table 2** Orthogonal test level parameters

| No | Preparation time (min) | Time ratio | Radius ratio | Intake pressure (MPa) | Speed ratio |
|---|---|---|---|---|---|
| 01 | 15 | 1:2 | 5:2 | 2 | 2:1 |
| 02 | 20 | 1:3 | 5:3 | 4 | 3:1 |
| 03 | 25 | 2:1 | 5:4 | 6 | 1:3 |
| 04 | 30 | 3:1 | 5:5 | 8 | 1:2 |

edges are generally asymmetric. Likewise, the asymmetric edges can be characterized by a form factor $K$ [5], $K = S_\alpha / S_\gamma$ (details are given in Fig. 17). At the same time, based on the tool passivation experiment platform of gas–solid two-phase flow abrasive particles, the orthogonal experiment was used to study the asymmetric cutting edge shape factor $K > 1$ and $K < 1$, the influence of passivation time, forward and reverse time ratio, intake pressure, radius ratio and rotational speed ratio on the front tool surface passivation value Sα, the back tool surface passivation value Sγ and the shape factor $K$ [].

The key controlling factors for form factor are preparation time, time ratio, radius ratio, intake pressure and speed ratio. Therefore, orthogonal milling experiment with five factors and four levels is adopted in this paper, as shown in Table 2. Subsequently, the orthogonal experiments for shape factor $K < 1$ and $K > 1$ are explained in Table 3.

## Analysis on Experiment Results

(1) Edge morphology

The edge morphology before and after edge preparation is presented in Figs. 18 and 19. As evident from the figures, surface defects, marks and burr were removed after the edge preparation.

(2) Abrasive state

Similarly, abrasive state before and after the air flow is presented in Fig. 20a–b. The abrasives were observed to be

**Table 3** Orthogonal experimental scheme

| | Time (min) | Time ratio | Radius ratio | Intake pressure (MPa) | Speed ratio | $K < 1$ | | | $K > 1$ | | |
|---|---|---|---|---|---|---|---|---|---|---|---|
| | | | | | | $S_\gamma$ (μm) | $S_\alpha$(μm) | $K$ | $S_\gamma$(μm) | $S_\alpha$(μm) | $K$ |
| 1 | 15 | 1:2 | 5:2 | 2 | 2:1 | 5.141 | 7.919 | 0.649 | 5.475 | 5.463 | 1.002 |
| 2 | 15 | 1:3 | 5:3 | 4 | 3:1 | 2.704 | 4.150 | 0.651 | 4.755 | 4.754 | 1.000 |
| 3 | 15 | 2:1 | 5:4 | 6 | 1:3 | 2.600 | 3.945 | 0.659 | 4.723 | 4.658 | 1.014 |
| 4 | 15 | 3:1 | 5:5 | 8 | 1:2 | 6.405 | 9.880 | 0.648 | 6.021 | 5.451 | 1.104 |
| 5 | 20 | 1:2 | 5:3 | 6 | 1:2 | 3.693 | 5.721 | 0.645 | 3.453 | 3.367 | 1.026 |
| 6 | 20 | 1:3 | 5:2 | 8 | 1:3 | 3.130 | 5.050 | 0.620 | 5.194 | 4.929 | 1.054 |
| 7 | 20 | 2:1 | 5:5 | 2 | 3:1 | 2.879 | 4.883 | 0.600 | 4.045 | 3.917 | 1.033 |
| 8 | 20 | 3:1 | 5:4 | 4 | 2:1 | 2.610 | 4.482 | 0.582 | 4.207 | 3.998 | 1.052 |
| 9 | 25 | 1:2 | 5:4 | 8 | 3:1 | 3.076 | 5.426 | 0.567 | 4.242 | 3.901 | 1.087 |
| 10 | 25 | 1:3 | 5:5 | 6 | 2:1 | 2.277 | 4.036 | 0.564 | 5.924 | 5.514 | 1.074 |
| 11 | 25 | 2:1 | 5:2 | 4 | 1:2 | 2.161 | 3.863 | 0.559 | 4.001 | 3.362 | 1.19 |
| 12 | 25 | 3:1 | 5:3 | 2 | 1:3 | 2.245 | 4.127 | 0.544 | 4.431 | 4.016 | 1.103 |
| 13 | 30 | 1:2 | 5:5 | 4 | 1:3 | 2.213 | 4.115 | 0.538 | 5.804 | 5.209 | 1.114 |
| 14 | 30 | 1:3 | 5:4 | 2 | 1:2 | 2.739 | 5.161 | 0.531 | 6.462 | 5.353 | 1.207 |
| 15 | 30 | 2:1 | 5:3 | 8 | 2:1 | 2.448 | 5.125 | 0.478 | 4.438 | 3.423 | 1.297 |
| 16 | 30 | 3:1 | 5:2 | 6 | 3:1 | 3.346 | 6.786 | 0.493 | 5.864 | 3.987 | 1.471 |

**Fig. 19** Edge morphology after edge preparation

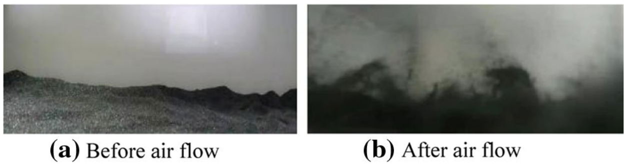


**Fig. 20** Abrasive state

in a static state initially; however, as the air starts flowing in, the abrasives enter a flow state.

(3) Extreme difference analysis for form factor $K < 1$

The results obtained through experiments are assessed using an extreme difference analysis [19]. Table 4 presents the impact of different parameters on form factor while $K < 1$. Based on extreme difference analysis, influence of each preparation parameter on the relevant form factor is investigated. Moreover, according to average values, the impact of different parameters on form factor is observed. The range analysis shows that the influence of parameters on the form factor is different.

From Table 4, in descending order of importance are the time ratio, the preparation time, the intake pressure, radius ratio and speed ratio. The maximum form factor is obtained using the following parameters: preparation time = 25 min, time ratio = 2:1, radius ratio = 5:5, intake pressure = 6 Mpa and speed ratio = 1:2.

Accordingly, influence of various parameters on the form factor, when $K < 1$, is given in Fig. 21. For preparation time, the form factor increases with increasing preparation time. The longer the preparation time, the higher the impact energy between the abrasive grain and the cutting edge,

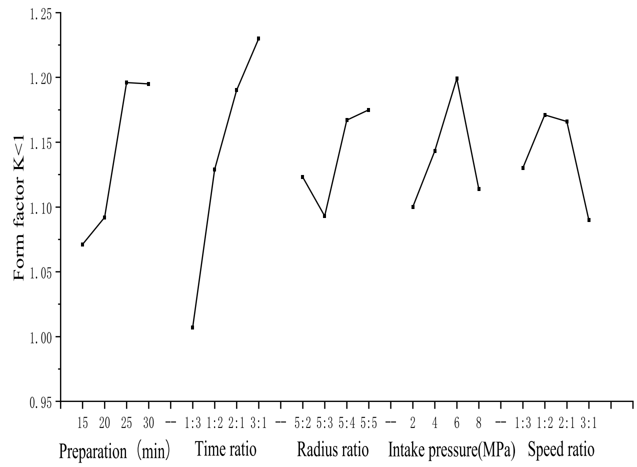


**Fig. 21** Influence of various parameters on the form factor (when $K < 1$)

the greater the preparation value of the front and back surfaces of the tool, and the shape factor gradually increases. Moreover, the shape factor increases linearly with the time ratio. With the increase in the positive and negative rotation time ratio, the impact velocity between the abrasive and the tool face is faster, and the preparation value of the tool face is larger and the shape factor is larger than that of the tool face. Likewise, the form factor first decreases with an increase in radius ratio. With the increase in the tool revolution radius, the rotation speed of the abrasive increases, and the abrasive and the tool will form a consistent relative motion. The higher the speed, the higher the collision energy of the abrasive, the larger the preparation value of the tool edge, the larger the shape factor, the reason for the decrease in the shape factor may be the result of experimental error. Similarly, with an increase in intake pressure, the form factor first increases and then decreases. When the intake pressure increases to a reasonable range, the number of abrasive particles increases, the impact energy value of abrasive particles on the cutting edge increases, the preparation effect is good, and the shape factor increases, but the intake pressure is too large, and the abrasive particles have no time to contact the cutting edge of the tool, the preparation effect is poor, and the shape factor decreases. Lastly, a

**Table 4** Extreme difference analysis of form factor (when $K < 1$)

| Extreme difference | Preparation time (min) | Time ratio | Radius ratio | Intake pressure (MPa) | Speed ratio |
|---|---|---|---|---|---|
| Mean 1 | 1.071 | 1.129 | 1.123 | 1.100 | 1.166 |
| Mean 2 | 1.092 | 1.007 | 1.093 | 1.143 | 1.090 |
| Mean 3 | 1.196 | 1.190 | 1.167 | 1.199 | 1.130 |
| Mean 4 | 1.195 | 1.230 | 1.175 | 1.114 | 1.171 |
| Range | 0.122 | 0.223 | 0.082 | 0.099 | 0.081 |

similar trend can be seen for the speed ratio where the form factor first increases and then decreases, with an increasing speed ratio. With the increase in speed ratio, the tool rotates too fast, the abrasive grain and the tool edge contact effect is poor, the tool preparation value decreases, and the shape factor decreases.

(4) Extreme difference analysis when form factor $K > 1$

To illustrate further, Table 5 presents the impact of each test parameter on corresponding form factor value, when $K > 1$. Table 5 illustrates that the main factors affecting the form factor when form factor $K > 1$; in descending order of importance are the time ratio, the intake pressure, the preparation time, speed ratio and radius ratio. The values of parameters corresponding to maximum form factor are preparation time = 30 min, time ratio = 3:1, radius ratio = 5:5, intake pressure = 6 Mpa, and speed ratio = 1:3.

The dependencies of preparation parameters with respective form factors (for $K > 1$) are plotted in Fig. 22. As evident from the graph, form factor increases with increasing preparation time. The longer the preparation time, the higher the impact energy between the abrasive and the cutting edge, the greater the preparation value of the tool front and rear surface, and the shape factor gradually increases. Furthermore, the form factor exhibits linear behavior with an increase in time ratio. With the increase in the positive and negative rotation time ratio, the impact velocity between the abrasive and the tool face is faster, and the preparation value of the tool face is larger and the shape factor is larger than that of the tool face. With increasing radius ratio, the form factor fluctuates back and forth, i.e., form factor first decreases, then increases and finally starts decreasing. With the increase in the tool revolution radius, the rotation speed of the abrasive increases, and the abrasive and the tool will form a consistent relative motion. The higher the speed, the higher the collision energy of the abrasive, the larger the preparation value of the tool edge, the larger the shape factor; the reason for the decrease in the shape factor may be the result of experimental error. Similarly, with increasing intake pressure, the form factor first increases and then starts decreasing. When the intake pressure increases to a reasonable

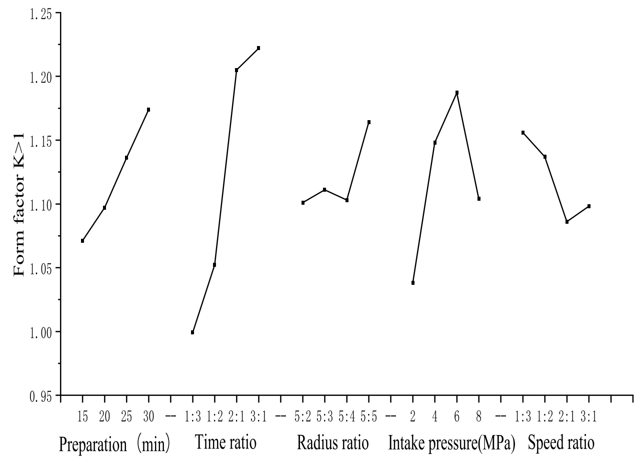


**Fig. 22** Influence of various parameters on the form factor (when $K > 1$)

range, the number of abrasive particles increases, the impact energy value of abrasive particles on the cutting edge increases, the preparation effect is good, the shape factor increases, but the intake pressure is too large, the abrasive particles have no time to contact the cutting edge of the tool, the preparation effect is poor, the shape factor decreases. Oppositely, as the speed ratio increases, the form factor first decreases and later on starts increasing. With the increase in speed ratio, the tool rotates too fast, the contact effect between the abrasive grain and the cutting edge is poor, the preparation value of the tool decreases, the shape factor decreases, and the shape factor suddenly increases, which may be the reason for the experimental error.

(5) Comparison of the measured form factor before and after edge preparation

The form factors measured before and after the edge preparation (when $K > 1$ and $K < 1$) are compared in Figs. 23 and 24, respectively. When $K < 1$, the form factor increases more rapidly than that before edge preparation, the maximum increased by 260%, and the minimum increased by 131%. When $K > 1$, some form factors increase more rapidly than that before edge preparation, while some factors decrease.

**Table 5** Extreme difference analysis of form factor (when $K > 1$)

| Extreme difference | Preparation time (min) | Time ratio | Radius ratio | Intake pressure (MPa) | Speed ratio |
|---|---|---|---|---|---|
| Mean 1 | 1.071 | 1.052 | 1.101 | 1.038 | 1.098 |
| Mean 2 | 1.097 | 0.999 | 1.111 | 1.148 | 1.086 |
| Mean 3 | 1.136 | 1.205 | 1.103 | 1.187 | 1.156 |
| Mean 4 | 1.174 | 1.222 | 1.164 | 1.104 | 1.137 |
| Range | 0.103 | 0.223 | 0.063 | 0.149 | 0.070 |

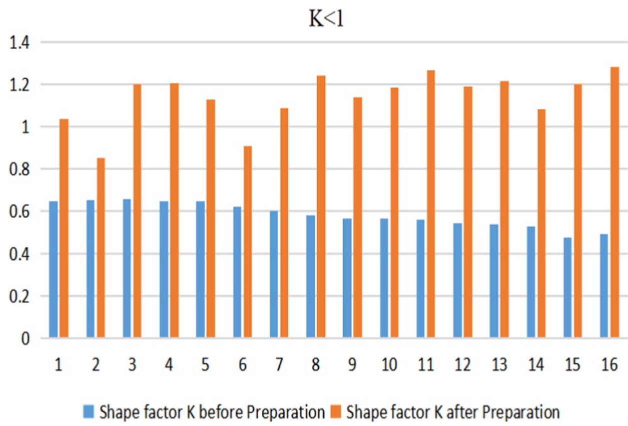


**Fig. 23** Influence of various parameters on the form factor (when $K<1$)

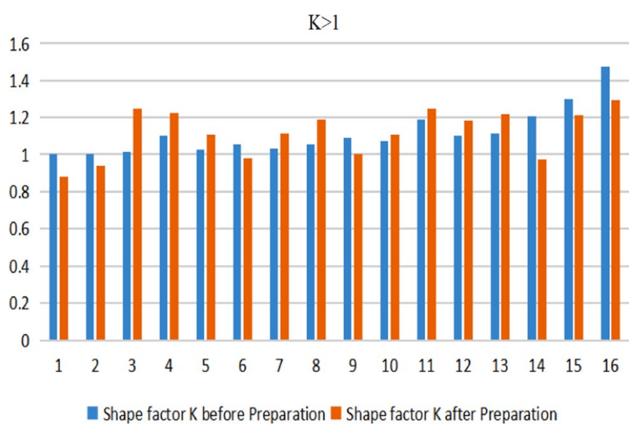


**Fig. 24** Influence of various parameters on the form factor (when $K>1$)

The maximum increased by 124%, while the maximum decreased by 123%. According to the extreme difference analysis, the time ratio is the main influence parameter on the form factor.

## Conclusion

In this paper, a gas–solid two-phase abrasive flow preparation is proposed. The simulation model is established to simulate the preparation process through coupled CFD and EDEM method. The experimental platform for tool edge preparation is developed based on gas–solid two-phase abrasive flow. Moreover, the orthogonal experiments are designed for the form factors $K<1$ and $K>1$, before preparation. The main conclusions of this work are as follows:

(1) In first 0.2 s of the initial stage, abrasives rise sharply and then settle to a certain height where they move in a relatively stable condition. The normal action force is observed to be greater than the tangential force, which highlights that material removal is mainly performed in the normal force action.

(2) The wear amount increases with increasing intake velocity. When the radius ratio is 5: 5, the impact on the edge is uniform, and the corresponding wear amount obtained is maximum. The wear amount and time ratio form a non-positive correlation relationship. Moreover, the effect of abrasive mesh on wear amount increases with increasing mesh.

(3) The critical factors affecting the form factor ($K<1$) are listed as (sorted in a descending order w.r.t their importance): time ratio, preparation time, intake pressure, radius ratio and speed ratio. Likewise, for $K>1$, the key controlling factors for form factor are listed as (sorted in a descending order w.r.t their importance): time ratio, intake pressure, preparation time, speed ratio and radius ratio.

(4) When $K<1$, the form factor increases more rapidly than that before edge preparation, where the increment in form factor ranges from 131 to 260%. Subsequently, for $K>1$, form factor increases in some cases more rapidly than that before edge preparation, while for other cases, the form factor decreases. For $K>1$, the maximum increment and decrement observed in form factor are 124% and 123%, respectively.

**Funding** This research was funded by National Natural Science Foundation Project (52065012 and 51665007).

**Declarations**

**Conflict of interest** The authors declare that they have no competing interest.

## References

1. M. Asad, Effects of tool edge geometry on chip segmentation and exit burr: a finite element approach. Metals **9**(11), 1234 (2019). https://doi.org/10.3390/met9111234
2. W. Wang, M.K. Saifullah, R. Aßmuth, D. Biermann, A.F.M. Arif, S.C. Veldhui, Effect of edge preparation technologies on cutting edge properties and tool performance. Int. J. Adv. Manuf. Technol. **106**(5), 1823–1838 (2020). https://doi.org/10.1007/s00170-019-04702-1
3. E. Uhlmann, D. Oberschmidt, Y. Kuche, A. Löwenstein, I. Winker, Effects of different cutting edge preparation methods on micro milling performance. Procedia CIRP **46**, 352–355 (2016). https://doi.org/10.1016/j.procir.2016.04.004
4. C.K. Aidun, Y. Lu, Lattice Boltzmann simulation of solid particles suspended in fluid. J. Stat. Phys. **81**(1–2), 49–61 (1995). https://doi.org/10.1007/BF02179967

5. B. Denkena, J. Köhler, C.E.H. Ventura, Customized cutting edge preparation by means of grinding. Precis. Eng. **37**(3), 590–598 (2013). https://doi.org/10.1016/j.precisioneng.2013.01.004
6. F. Xie, Z.S. Wu, Numerical simulation and experimental study of gas-solid two-phase flow in venturi tubes. J. Power Eng. **27**(2), 237–241 (2007). https://doi.org/10.1016/S1001-8042(07)60056-6
7. J.H. Walther, P. Koumoutsakos, Three-dimensional vortex methods for particle-lad n flows with two-way coupling. J. Comput. Phys. **167**(1), 49–61 (2001). https://doi.org/10.1006/jcph.2000.6656
8. O. Filippova, D. Hänel, Lattice-Boltzmann simulation of gas-particle flow in filter. Comput. Fluids **26**(7), 697–712 (1997). https://doi.org/10.1016/S0045-7930(97)00009-1
9. A.J.C. Ladd, Numerical simulations of particulate suspensions via a discretized Boltzmann equation. Part 1. Theoretical foundation. Fluid Mech. **271**, 285–309 (1994). https://doi.org/10.1017/s0022112094001771
10. L. Junye, S. Ningning, H. Jinglei, Y. Zhaojun, S. Liang, Z. Xinming, Numerical analysis and experiment of abrasive flow microhole machining based on CFD-DEM coupling. Trans. Chin. Soc. Agric. Eng. **34**(16), 80–88 (2018). https://doi.org/10.11975/j.issn.1002-6819.2018.16.011
11. B. Mikó, B. Palásti-Kovács, S. Sipos, Á. Drégelyi-Kiss, Investigation of cutting edge preparation for twist drills. Int. J. Mach. Mach. Mater. **17**(6), 529–542 (2015). https://doi.org/10.1504/IJMMM.2015.073722
12. D. Biermann, R. Aßmuth, S. Schumann, M. Rieger, B. Kuhlenkötter, Wet abrasive jet machining to prepare and design the cutting edge micro shape. Procedia CIRP **45**, 195–198 (2016). https://doi.org/10.1016/j.procir.2016.02.071
13. T. Bergs, S.A.M. Schneider, M. Amara, P. Ganser, Preparation of symmetrical and asymmetrical cutting edges on solid cutting tools using brushing tools with filament-integrated diamond grits. Procedia CIRP **93**, 873–878 (2020). https://doi.org/10.1016/j.procir.2020.04.028
14. C.E.H. Ventura, J. Köhler, B. Denkena, Cutting edge preparation of PCBN inserts by means of grinding and its application in hard turning. CIRP J. Manuf. Sci. Technol. **6**(4), 195–198 (2013). https://doi.org/10.1016/j.cirpj.2013.07.005
15. J. Wang, Q. Qiu, X. He, Numerical simulation of multiphase flow mixing in a stirred tank based on EDEM-fluent coupling. J. Zhengzhou Univ. (Eng. Sci.) **39**(05), 79–84 (2018). https://doi.org/10.13705/j.issn.1671-6833.2018.05.015
16. Y. Du, *Study on the Passivation of Carbide End Mill by Abrasive Particles* (Guizhou University, Guiyang, 2019)
17. W. Liu, *Study on the Influence of Planetary Motion Passivation on Tool Edge Morphology* (Guizhou University, Guiyang, 2017)
18. Y. Zou, D. Wen, Y. Wang, Y. Xiao, L. Zou, Numerical simulation and experimental study of ultrasonic vibration finishing based on EDEM. China Mech. Eng. **31**(06), 647–654 (2020)
19. R. Zhao, Y. Jiao, C. Zhu, Research on new beef pancake processing technology based on range analysis and principal component analysis. Mod. Food Sci. Technol. **35**(11), 8 (2019). https://doi.org/10.13982/j.mfst.1673-9078.2019.11.021